

Femtosecond laser ablation of polystyrene: A molecular dynamics study

Yanhua Huang,¹ Chengwei Song,¹ Junjie Zhang,² Tao Sun²

¹Research Center of Laser Fusion, China Academy of Engineering Physics, Mianyang 621900, China

²Center for Precision Engineering, Harbin Institute of Technology, Harbin 150001, China

Correspondence to: J. Zhang (E-mail: zhjj505@gmail.com)

ABSTRACT: In this work we perform molecular dynamics simulations to investigate the thermodynamic mechanisms of amorphous polystyrene ablated by a femtosecond laser pulse. The utilized width and fluence of the laser pulse are 10 fs and 10^{12} W/cm², respectively. Furthermore, the effect of chain length on the microscopic material removal mechanisms and related macroscopic evolutions of system quantities is studied. Simulations results indicate that the ultra-short laser pulse irradiation introduces significant instabilities into the target material because of the lattice perturbation, which leads to the relaxation of lattice destabilizations after the pulse through evaporation from the top surface and expansion within the bulk. It is found that the competition between the two mechanisms of evaporation and expansion is strongly influenced by the chain length. © 2015 Wiley Periodicals, Inc. *J. Appl. Polym. Sci.* 2015, 132, 42713.

KEYWORDS: mechanical properties; manufacturing; theory and modeling

Received 19 March 2015; accepted 5 July 2015

DOI: 10.1002/app.42713

INTRODUCTION

The polystyrene hollow microsphere is one of the most important targets used for the inertial confinement fusion, because it can decrease the instability of preheated fuel and hydromechanics in the course of radiant drive implosion.^{1–3} Particularly in the fast ignition scheme, a small gold cone is imbedded into a polystyrene microsphere to provide a clear pathway for ultra-tense laser to reach central region.⁴ Thus, a hole with micrometer dimensions is needed to be fabricated on polystyrene microsphere in advance of the imbedding of a gold cone. To avoid radial laser propagation in plasma, the machining accuracy of the hole is crucial to achieve accurate mating between the gold cone and the polystyrene microsphere. Therefore, how to accurately fabricate the hole on polystyrene microsphere becomes challenging.^{5–7}

Recently, the technique of femtosecond (fs) laser ablation has been proposed to fabricate a hole on polystyrene microsphere.^{8,9} However, till now the underlying physical mechanisms involved in the femtosecond laser ablation of polystyrene remain poorly understood, which greatly hinders the development of the machining ability. Typically, the femtosecond laser ablation is composed of two sequential stages, as (1) laser pulse irradiation with time scale of fs, in which laser energy is adsorbed by electrons, and (2) absorbed energy dissipation with time scale of picosecond (ps), which leads to material removals.^{10,11} Given

the involved ultra-short time scale, it's extremely difficult for experiments to monitor the phenomena occurred during the ongoing process of laser ablation. Furthermore, understanding the fundamental deformation behavior of polystyrene specimen under laser ablation processes requiring identification and distinguishing of inter-chain and intra-chain interactions, which are occurred in the atomic length scale. Therefore, the capability of monitoring and analyzing motions of single chains at atomic scale is critical to elucidate the thermodynamic mechanisms of polystyrene specimen under femtosecond laser ablation. On the theoretical side, the time steps used in molecular dynamics (MD) simulation are on the order of 1 fs, which fall into the length scale of the femtosecond laser ablation. Furthermore, it has been demonstrated that MD simulation can provides atomic information of the ongoing laser ablation processes.^{12–15} Particularly for the polystyrene, which is one typical long chain vinyl polymer with a phenyl group attached to every other carbon atom, the capability of monitoring and analyzing motions of single chains at atomic scale is critical to elucidate the underlying mechanisms of polystyrene specimen under laser ablation. However, MD simulation of the femtosecond laser ablation of polystyrene is rather scarce. Therefore, in this work we perform MD simulations to reveal the thermodynamic atomic mechanisms involved in the femtosecond laser ablation of amorphous polystyrene. The influence of chain length on the femtosecond laser ablation is further studied.

EXPERIMENTAL

Figure 1 presents the MD model of femtosecond laser ablation of polystyrene, which consists of an amorphous polystyrene target and an external laser field, which was also used in our recent work.¹⁶ The target consists of randomly assembled Atactic polystyrene chains, and has a dimension of $l_1 = 8$ nm, $l_2 = 16$ nm, and $l_3 = 8$ nm in X, Y, and Z direction, respectively. The density of polystyrene target can be calculated using eq. (1):

$$\rho = \frac{m}{V} = \frac{N \times (C_m \times 8n + H_m \times (8n + 2))}{l_1 \times l_2 \times l_3} \quad (1)$$

Where N is the chain length, $C_m = 1.9927e^{-26}$ kg and $H_m = 1.6606e^{-27}$ kg are atomic masses for single carbon and hydrogen atoms, respectively. Accordingly, the as-created polystyrene target has a density of approximate 814.7 kg/m³. Periodic boundary conditions are imposed in the lateral X and Z directions, while the Y direction of the target is kept free. Furthermore, the bottom of the target with the length of 1 nm is fixed during the whole laser ablation process. As depicted in Figure 1, the length of the laser irradiated region is 12 nm. To investigate the influence of chain length on the laser ablation process, three targets with different chain lengths of 5, 10, and 20 are considered. Table I lists the detailed configurations for each target. The inter-molecular and intra-molecular interactions in the simulated polystyrene target are described by using the well-established AIREBO (Adaptive Intermolecular Reactive

Table I. Configuration Parameters for Polystyrene Targets with Different Chain Lengths

	Chain length	Number of chains	Atom number
Target1	5	976	80032
Target2	10	488	79056
Target3	20	244	78568

Empirical Bond Order) potential,¹⁷ which has been successfully used in our previous studies.¹⁸

The femtosecond laser ablation of polystyrene consists of two stages, as short-duration stage of laser pulse irradiation and subsequent long-duration stage of adsorbed energy dissipation. In the first stage, the femtosecond laser pulse irradiates the target from the top. The width and the fluence of the laser pulse are 10 fs and 10^{12} W/cm², respectively. In this work we mainly focus on the thermodynamic phenomena of the polystyrene target induced by laser ablation. Therefore, the laser energy is deposited into the laser irradiated region of the target homogeneously through velocity scaling, and the case of ionization is not considered. After the laser pulse, the polystyrene target is allowed to perform energy dissipation for 10 ps in the second stage. All the MD simulations are completed with the LAMMPS (Large-scale Atomic/Molecular Massively Parallel Simulator) code with a timestep of 0.1 fs.¹⁹ The VMD (Visual Molecular Dynamics) is utilized to visual MD calculation date and generate MD snapshots.²⁰

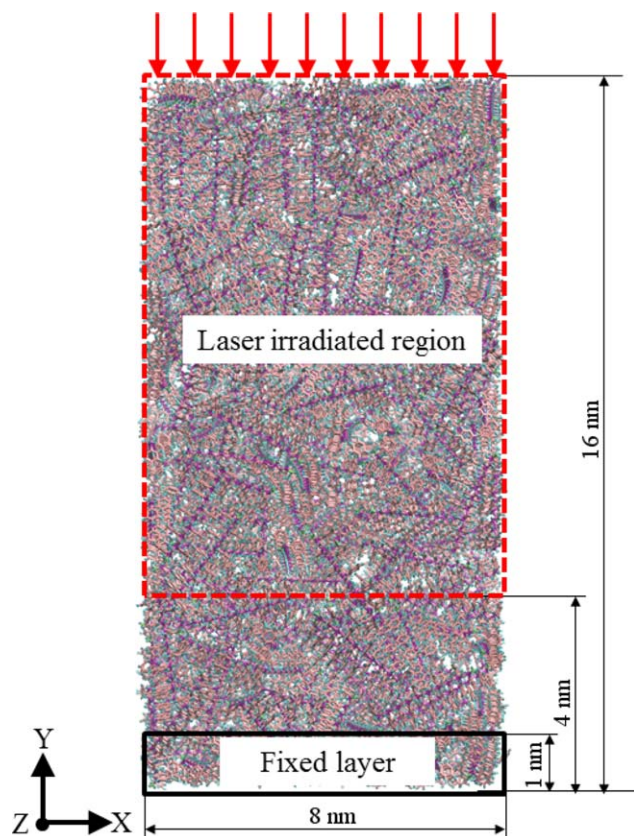


Figure 1. MD model of femtosecond laser ablation of amorphous polystyrene. [Color figure can be viewed in the online issue, which is available at wileyonlinelibrary.com.]

RESULTS AND DISCUSSION

Mechanisms of Femtosecond Laser Ablation of Polystyrene

Before subjected to laser pulse irradiation, the atoms in the target has reached their equilibrium configurations at pressure of 0 bar and low temperature of 30 K, and the velocities of the atoms and the kinetic energy of the system are both kept as zero. In the stage of laser pulse irradiation, kinetic energy is added to the atoms in the laser irradiated region of the target with constant rate. Figure 2 plots the evolution of the scaled

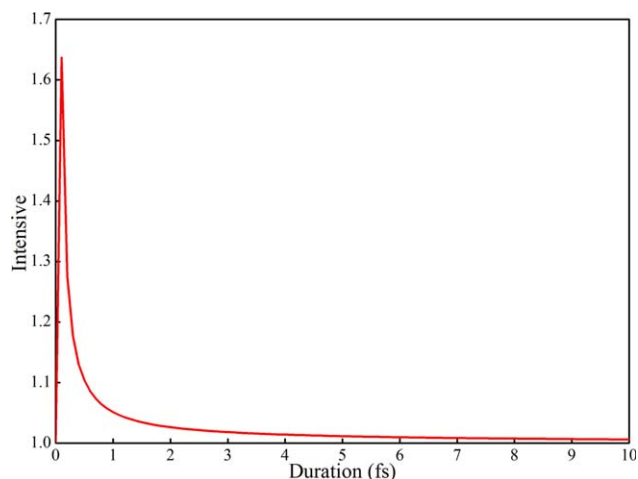


Figure 2. Evolution of scaled laser intensive during laser irradiation of the Target2. [Color figure can be viewed in the online issue, which is available at wileyonlinelibrary.com.]

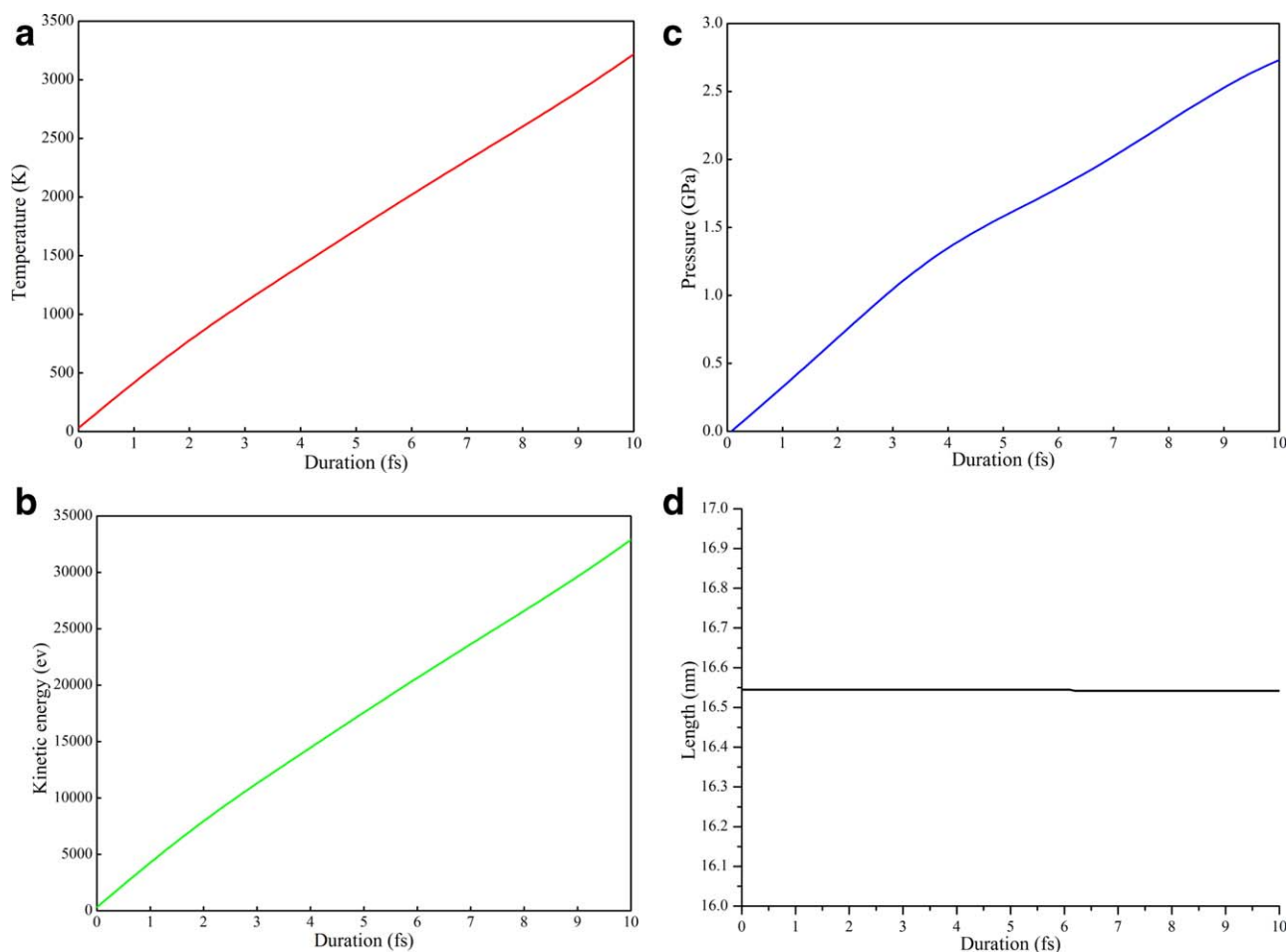


Figure 3. Evolutions of statistical quantities of the simulated system during laser irradiation of the Target2. (a) Temperature; (b) Kinetic energy; (c) Pressure; (d) Length. [Color figure can be viewed in the online issue, which is available at wileyonlinelibrary.com.]

laser intensive by the velocities of irradiated atoms with the duration for the Target2. The intensive first increases linearly to its maximum of 1.64, then drops precipitously upon further irradiation, and finally reaches a stable value approaching 1.0. To reveal the possible reasons for the observed characteristics of the intensive evolution, Figure 3 presents the evolutions of statistical quantities of the simulated system. It is seen from Figure 3(a) that the temperature of the Target2 increases approximately linearly under the laser irradiation, and finally reaches a value of 3218 K after the laser pulse. On a microscopic scale, the temperature increase corresponds to an increase of atomic kinetic energy. Accordingly, Figure 3(b) shows that the kinetic energy also increases dramatically.

The addition of the kinetic energy excites the atoms in the top-layer of the target, the velocities of which first increase rapidly from zero to their maximum values in the ultra-short duration of 0.2 fs, leading to the linear increase of the laser intensive shown in Figure 1. Upon further irradiation, however, the sub-layer of the target is also irradiated by the laser pulse, the increase of the number of averaged atoms leads to the decrease of the laser intensive, in spite of the monotonous increase of the kinetic energy. It is seen from Figure 3(c) that the irradiation

leads to considerable compressive stress existed in the material, evidenced by the positive value of pressure. However, Figure 3(d) demonstrates that the irradiation of single laser pulse doesn't result in significant modification of the target, due to the ultra-short time scale of the laser pulse.^{10,11}

The irradiation of the short laser pulse introduces instabilities into the target because of the perturbation of the target lattices. After the laser pulse, those lattice destabilizations are relaxed accompanied by the ablation of the target material. Be similar with the stage of laser pulse irradiation, Figure 4 presents the evolutions of statistical quantities of the simulated system during the stage of adsorbed energy dissipation. Figure 4(a,b) show that both the temperature and kinetic energy of the system first decrease precipitously within the initial duration of 0.1 ps, followed by gentle evolution. Furthermore, in the later duration both the temperature and the kinetic energy of the system increase slightly. Accompanied with the dissipation of adsorbed energy, Figure 4(c) shows that the pressure of the system first drops dramatically, and then gradually reaches stable value that approaches zero, indicating the complete relaxation of the compressive stresses accumulated in the stage of laser pulse irradiation. It is seen from Figure 4(d) that the evolution of the length

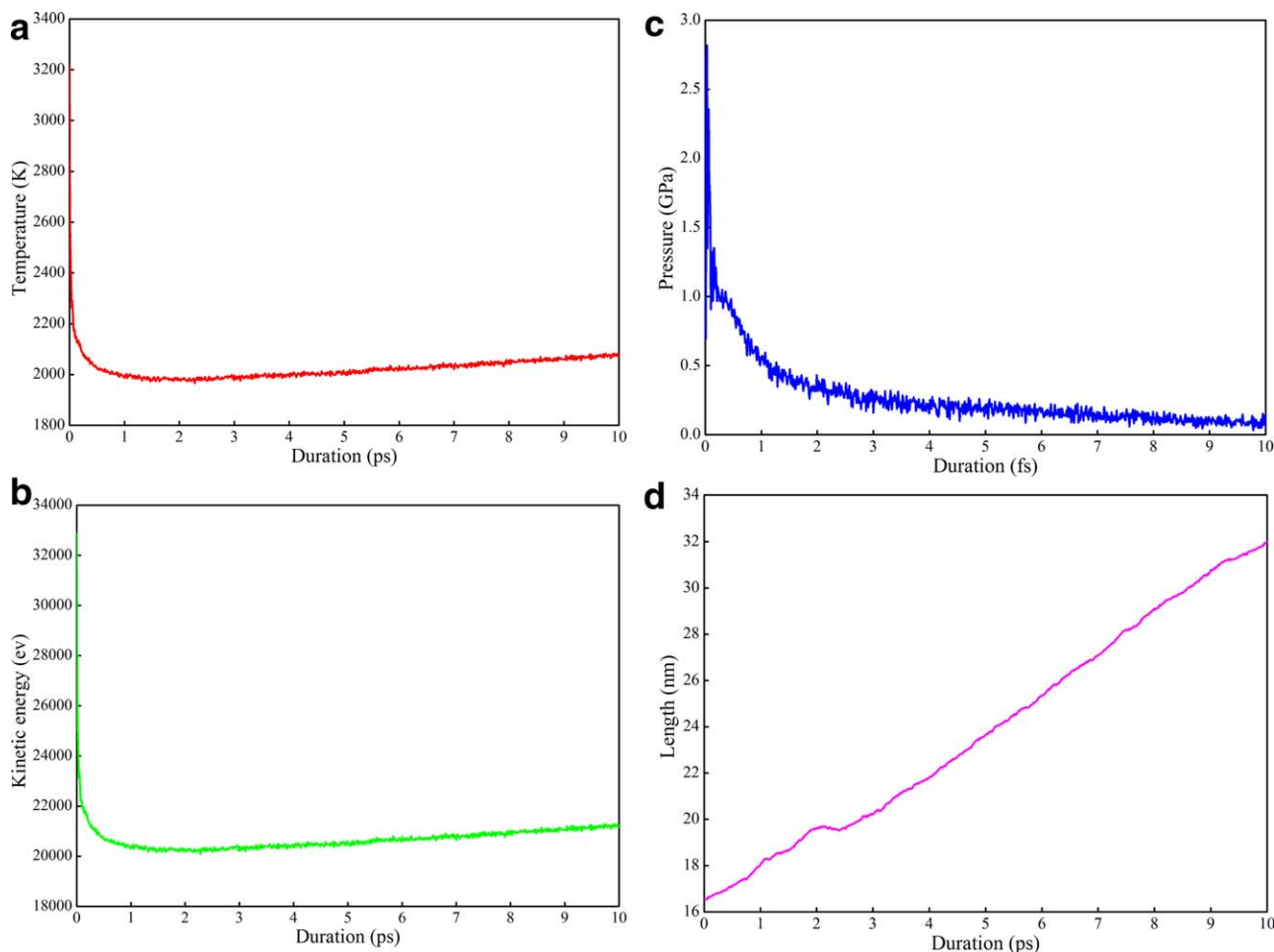


Figure 4. Evolutions of statistical quantities of the simulated system during adsorbed energy dissipation of the Target2. (a) Temperature; (b) Kinetic energy; (c) Pressure; (d) Length. [Color figure can be viewed in the online issue, which is available at wileyonlinelibrary.com.]

can be divided into two zones, according to the characteristics shown in the length-duration curve. In the first zone the length increases with strong fluctuations, which in accordance with the significant change of the system quantities in the initial period of the adsorbed energy dissipation. After the first zone, the length increases approximately linearly in the second zone. The length of the system finally reaches 32.0 nm, increased by 50% in comparison with its initial value before the adsorbed energy dissipation.

Figure 5 presents MD snapshots of the Target2 undergoing adsorbed energy dissipation at different durations. Figure 5(a) shows that the polystyrene chains are assembled closely, although there is considerable adsorbed energy existed in the top layer of the target. Figure 5(b–e) demonstrate that the evolution of the target material induced by the energy dissipation can be divided into two types, as evaporation from the top surface and expansion within the bulk. While the evaporation of the material introduces tensile stress into the system, the expansion within the bulk leads to further increase of the compressive stress. In the initial period of the adsorbed energy dissipation, the evaporation rather than the expansion dominates the ablation of the material, thus the pressure of the system drops

dramatically as indicated by Figure 4(c). The close inspection of the evolution of individual chains demonstrates that accompanied with the evaporation, the chains also undergo significant evolution such as interchain-sliding and intrachain-change. Particularly, the intrachain-change enables the chains reaching their energy favorable local equilibrium configurations, which consequently leads to the fluctuations of the increased length.¹⁹ However, upon further propagation of the adsorbed energy from the top surface to the rear bottom of the target, the expansion of chains within the bulk becomes more pronounced. Furthermore, the increased number of evaporated chains increases the possibilities of collisions between each other. Therefore, both of the temperature and the kinetic energy increase slightly in the latter period of the adsorbed energy dissipation. The strong competition between the evaporation and expansion erases the fluctuations observed in the initial period, leading to a linear increase of the length.¹⁶

Influence of Chain Length

With the insights into the mechanisms of femtosecond laser ablation obtained in the Section 3.1, the influence of chain length on the femtosecond laser ablation is investigated. The detailed configuration of the three targets is presented in

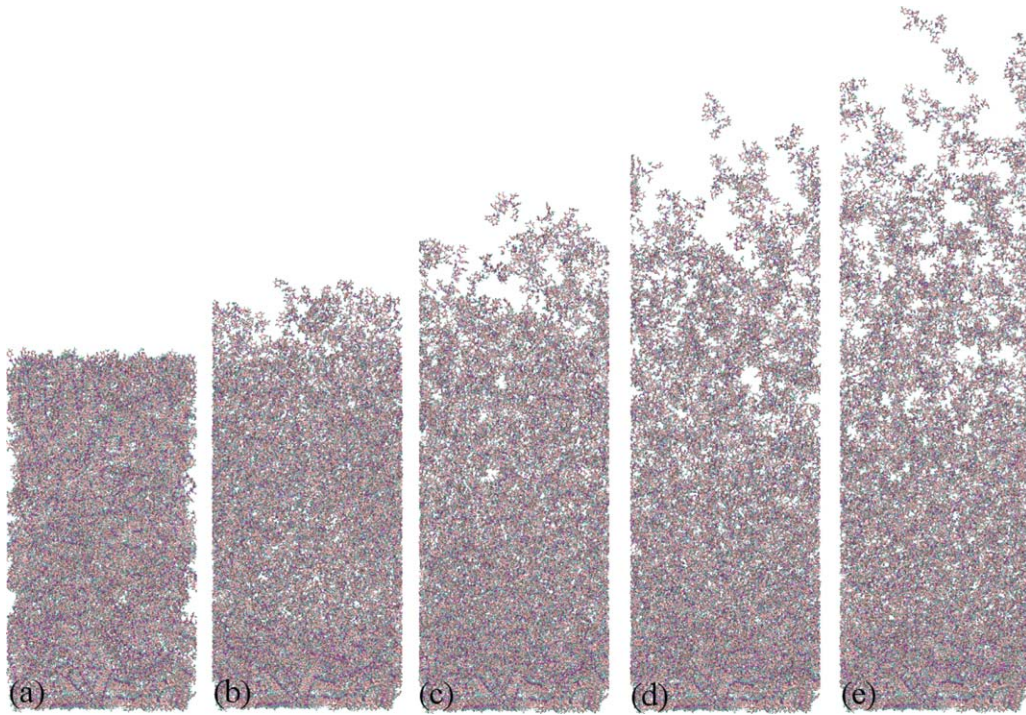


Figure 5. MD snapshots of the Target2 during the stage of adsorbed energy dissipation. Duration: (a) 0 ps, (b) 2.5 ps, (c) 5.0 ps, (d) 7.5 ps, and (e) 10.0 ps. [Color figure can be viewed in the online issue, which is available at wileyonlinelibrary.com.]

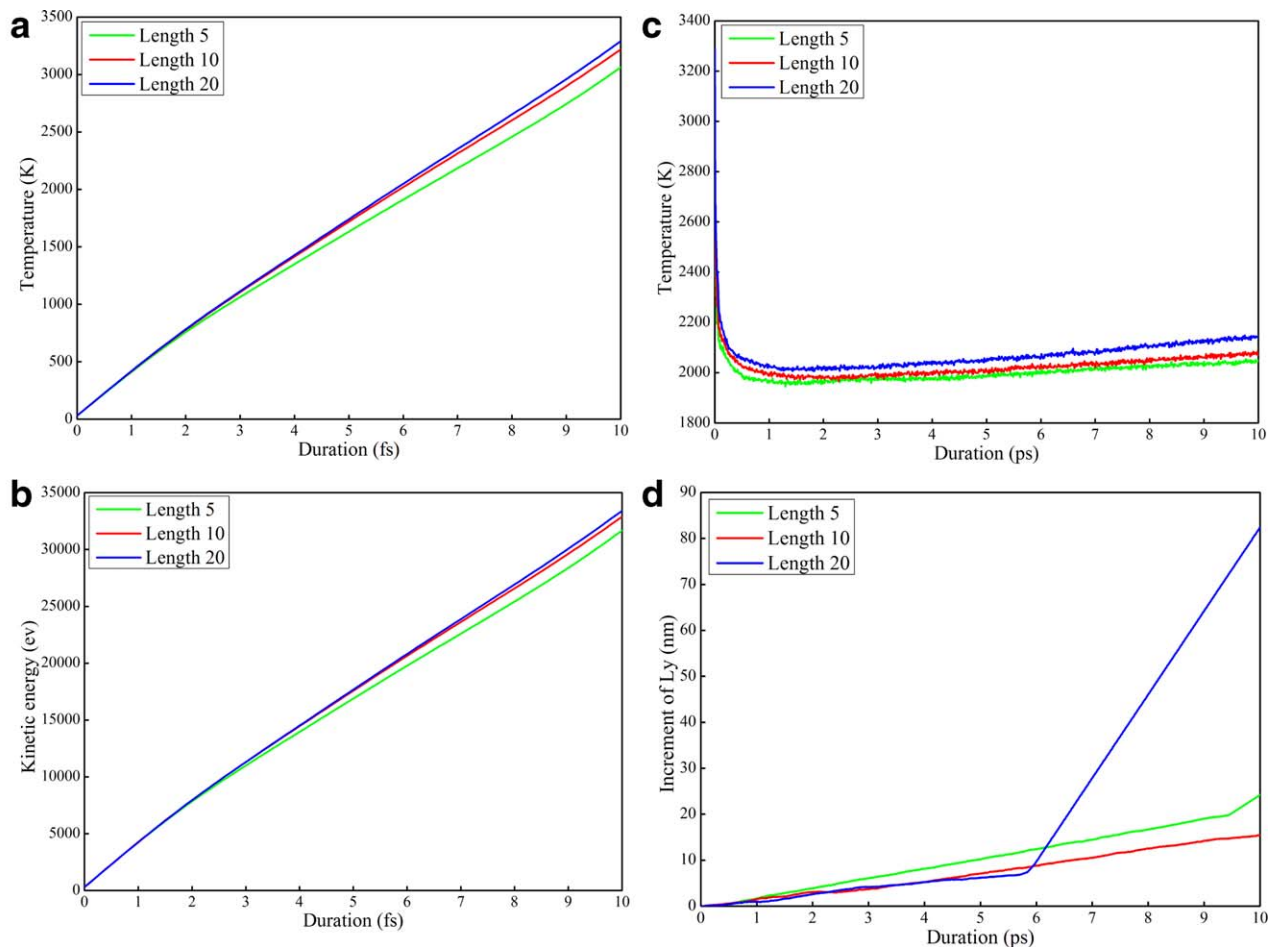


Figure 6. Influence of chain length on the evolutions of statistical quantities of the system during laser ablation of different targets. Stage of laser pulse irradiation: (a) Temperature; (b) Kinetic energy; Stage of adsorbed energy dissipation: (c) Temperature; (d) Increment of length. [Color figure can be viewed in the online issue, which is available at wileyonlinelibrary.com.]

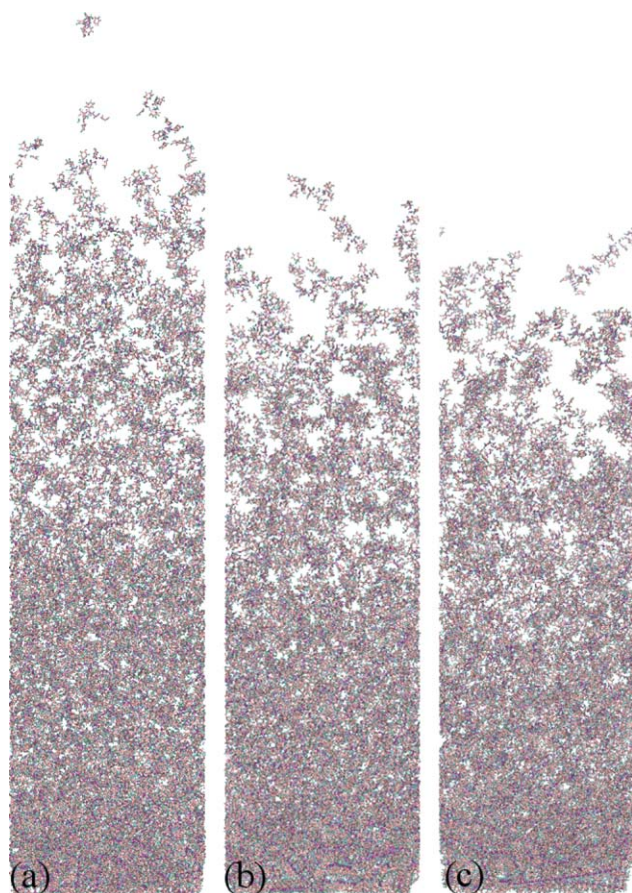


Figure 7. MD snapshots of three targets after the completion of the stage of adsorbed energy dissipation. (a) Target1, (b) Target2, (c) Target3. [Color figure can be viewed in the online issue, which is available at wileyonlinelibrary.com.]

Table I. Figure 6(a,b) plot the temperature-duration curves and kinetic energy-duration curves for the three targets during the stage of laser pulse irradiation, respectively. It is seen from Figure 6 that the evolutions of both temperature and kinetic energy has similar characteristics, as monotonously increase with increasing duration. However, the larger the chain length, the higher the slopes of both the temperature-duration curves and the kinetic energy-duration curves.

Figure 6(c) plots the temperature-duration curves for the three chain lengths under adsorbed energy dissipation. For each chain length, the temperature first drops precipitously due to significant evaporation from the top surface of the target, and then increases slightly due to more pronounced expansion within the bulk. Furthermore, the temperature-duration curve for the large chain length is above of that for the small chain length. In contrast, Figure 6(d) demonstrates that the increment of the length is smaller for the larger chain length. We note that the rapid increase of the length for the Target3 with the largest chain length from the duration of 5.8 ps is caused by the formation of separated atoms because of the broken of polymer chain bonds, which escape far away from the top surface. However, since the quantity of the separated atoms is rather limited, in this work we do not consider its impact on the evolution of the system quantities.

Figure 7 presents MD snapshots of the three targets after the completion of adsorbed energy dissipation. It is seen from Figure 7 that evaporation from the top surface and expansion within the bulk are the two mechanisms operating in the three targets. However, the competition between the two mechanisms is strongly influenced by chain length. For the small chain length, the evaporation dominates the ablation of the material because of the small molecule weight. For the large chain length corresponding large molecule weight, however, large energy is required for the evaporation of the chains from the top surface due to the entanglement of the long polystyrene chains.^{21–24} Furthermore, the bulk material with larger chain length is more difficult to be excited within the bulk. Figure 7 also demonstrates that the density of the bulk material in the vicinity of the fixed bottom increases with increasing chain length.

CONCLUSIONS

In summary, in the present study we elucidate the thermodynamic mechanisms operating in the amorphous polystyrene under femtosecond laser ablation by means of MD simulations. The utilized laser pulse width and fluence are 10 fs and 10^{12} W/cm², respectively. Our results demonstrate that MD simulation with full atomic resolution is powerful to elucidate the fundamental thermodynamic mechanisms of polystyrene under laser ablation at the atomic scale. Although the target volume remains nearly unchanged in the short-duration of laser pulse irradiation, there are considerable instabilities associated with compressive stress existed in the material, due to lattice perturbations. The subsequent relaxation of those lattice destabilizations after the pulse is achieved by the two competitive mechanisms, as evaporation from the top surface and expansion within the bulk. It is found that the chain length has strong influence on the ablation of the target. When chain length is small, the evaporation dominates the ablation and consequently the volume change is large. For the large chain length, however, expansion becomes more pronounced than evaporation because of larger molecule weight.

ACKNOWLEDGMENTS

This work was financially supported by the National Natural Science Foundation of China under Grant No.51006093 and by Laboratory of Precision Manufacturing Technology, China Academy of Engineering Physics under Grant No.zz13010.

REFERENCES

- Zhang, L.; Cui, B.; Zhou, L.; Yuan, Y. *High Power Laser Particle Beams* **1995**, *7*, 151.
- Mishra, K. K.; Khardekar, R. K.; Singh, R.; Pant, H. C. *Pramana – J. Phys.* **2002**, *59*, 113.
- Bin, W.; Shujun, W.; Hongguang, S.; Hongyan, L.; Jie, L.; Ning, L. *Petroleum Sci.* **2009**, *6*, 306.
- Kodama, R.; Norreys, P. A.; Mima, K.; Dangor, A. E.; Evans, R. G.; Fujita, H.; Kitagawa, Y.; Krushelnick, K.; Miyakoshi, T.; Miyanaga, N.; Norimatsu, T.; Rose, S. J.; Shozaki, T.; Shigemori, K.; Sunahara, A.; Tampo, M.; Tanaka, K. A.; Toyama, Y.; Yamanaka, T.; Zepf, M. *Nature* **2001**, *412*, 798.

5. Hill, D. W.; Castillo, E.; Chen, K. C.; Grant, S. E.; Greenwood, A. L.; Kaae, J. L.; Nikroo, A.; Paguio, S. P.; Shearer, C.; Jr.; Smith, J. N.; Stephens, R. B.; Steinman, D. A.; Wall, J. *Fusion Sci. Technol.* **2004**, *45*, 113.
6. Mishra, K. K.; Khardekar, R. K.; Singh, R.; Pant, H. C. *Pramana* **2002**, *59*, 113.
7. Yang, W. B.; Zhang, B. J.; Dai, Y. T.; Tang, X. H.; Zhang, L. *Fusion. Eng. Des.* **2008**, *83*, 725.
8. Homma, H.; Kodota, H.; Hosokawa, H. *Fusion Sci. Technol.* **2011**, *59*, 276.
9. Nagai, K.; Yang, H.; Norimatsu, T. *Nucl. Fusion.* **2009**, *49*, 1.
10. Miotello, A.; Ossi, P. M., Eds. *Laser-Surface Interactions for New Materials Production*, Springer Ser. Mat. Sci.: Berlin/Heidelberg, **2010**; p 19.
11. Jiang, L.; Tsai, H. L. In *Proceedings of NSF Workshop on Research Needs in Thermal, Aspects of Material Removal*, Stillwater, OK, **2003**.
12. Wang, Y.; Xu, X.; Zhang, L. *Appl. Phys. A* **2008**, *92*, 849.
13. Perez, D.; Lewis, L. *J. Phys. Rev. B* **2003**, *67*, 184102.
14. Sonntag, S.; Paredes, C. T.; Roth, J.; Trebin, H. R. *Appl. Phys. A* **2011**, *104*, 559.
15. Upadhyay, A. K.; Inogamov, N. A.; Rethfeld, B.; Urbassek, H. M. *Phys. Rev. B* **2008**, *78*, 045437.
16. Huang, Y. H.; Song, C. W.; Zhang, J. J.; Sun, T. *Sci China-Phys Mech Astron* **2015**, *58*, 037002.
17. Stuart, S. J.; Harrison, J. A.; Tutein, A. B. *J. Chem. Phys.* **2000**, *112*, 6472.
18. Du, K.; Tang, Y. J.; Zhang, J. J.; Xu, F. D.; Yan, Y. D.; Sun, T. *Curr. Nanosci.* **2013**, *9*, 153.
19. Plimpton, S. J. *Comput. Phys.* **1995**, *117*, 1.
20. Humphrey, W.; Dalke, A.; Schulten, K. *J. Mol. Graphics* **1996**, *14*, 33.
21. Brian, P. C.; Torkelson, J. M. *Macromolecules* **2002**, *35*, 8126.
22. Yifu, D.; Novikov, V. N.; Sokolov, A. P.; Cailliaux, A.; Dalle-Ferrier, C.; Alba-Simionesco, C.; Frick, B. *Macromolecules* **2004**, *37*, 9264.
23. Rebollar, E.; Bounos, G.; Selimis, A.; Castillejo, M.; Georgiou, S. *Appl. Phys. A* **2008**, *92*, 1043.
24. Zhigilei, L. V.; Leveugle, E.; Sellinger, A.; Fitz-Gerald, J. M. *Proc. SPIE* **2008**, *7005*, 700517.